

The Stellar $^{72}\text{Ge}(n, \gamma)$ Cross Section for weak s-process: A First Measurement at n_TOF

M. Dietz^{1,2,*}, C. Lederer-Woods¹, A. Tattersall¹, U. Battino¹, F. Gunsing^{3,4}, S. Heinitz⁵, M. Kr̄t̄icka⁶, J. Lerendegui-Marco⁷, R. Reifarh⁸, S. Valenta⁶, O. Aberle⁴, S. Amaducci^{9,10}, J. Andrzejewski¹¹, L. Audouin¹², M. Bacak^{13,4,3}, J. Balibrea¹⁴, M. Barbagallo¹⁵, F. Bečvár⁶, E. Berthoumieux³, J. Billowes¹⁶, D. Bosnar¹⁷, A. Brown¹⁸, M. Caamaño¹⁹, F. Calviño²⁰, M. Calviani⁴, D. Cano-Ott¹⁴, R. Cardella⁴, A. Casanovas²⁰, F. Cerutti⁴, Y. H. Chen¹², E. Chiaveri^{4,16,7}, N. Colonna¹⁵, G. Cortés²⁰, M. A. Cortés-Giraldo⁷, L. Cosentino²¹, L. A. Damone^{15,22}, M. Diakaki³, C. Domingo-Pardo²³, R. Dressler⁵, E. Dupont³, I. Durán¹⁹, B. Fernández-Domínguez¹⁹, A. Ferrari⁴, P. Ferreira²⁴, P. Finocchiaro²¹, K. Göbel⁸, A. R. García¹⁴, A. Gawlik-Ramięga¹¹, S. Gilardoni⁴, T. Glodariu^{†25}, I. F. Gonçalves²⁴, E. González-Romero¹⁴, E. Griesmayer¹³, C. Guerrero⁷, H. Harada²⁶, J. Heyse²⁷, D. G. Jenkins¹⁸, E. Jericha¹³, F. Käppeler^{†28}, Y. Kadi⁴, D. Kahl¹, A. Kalamara²⁹, P. Kavrigin¹³, A. Kimura²⁶, N. Kivel⁵, M. Kokkoris²⁹, M. Kr̄t̄icka⁶, D. Kurtulgil⁸, E. Leal-Cidoncha¹⁹, H. Leeb¹³, S. Lo Meo^{30,9}, S. J. Lonsdale¹, D. Macina⁴, A. Manna^{9,10}, J. Marganec^{11,2}, T. Martínez¹⁴, A. Masi⁴, C. Massimi^{9,10}, P. Mastinu³¹, M. Mastroarco¹⁵, E. A. Mauger⁵, A. Mazzone^{15,32}, E. Mendoza¹⁴, A. Mengoni³⁰, P. M. Milazzo³³, F. Mingrone⁴, A. Musumarra^{21,34}, A. Negret²⁵, R. Nolte², A. Oprea²⁵, N. Patronis³⁵, A. Pavlik³⁶, J. Perkowski¹¹, I. Porras³⁷, J. Praena³⁷, J. M. Quesada⁷, D. Radeck², T. Rauscher^{38,39}, C. Rubbia⁴, J. A. Ryan¹⁶, M. Sabaté-Gilarte^{4,7}, A. Saxena⁴⁰, P. Schillebeeckx²⁷, D. Schumann⁵, A. G. Smith¹⁶, N. V. Sosnin¹⁶, A. Stamatopoulos²⁹, G. Tagliente¹⁵, J. L. Tain²³, A. Tarifeño-Saldivia²⁰, L. Tassan-Got¹², G. Vannini^{9,10}, V. Variale¹⁵, P. Vaz²⁴, A. Ventura⁹, V. Vlachoudis⁴, R. Vlastou²⁹, A. Wallner⁴¹, S. Warren¹⁶, C. Weiss¹³, P. J. Woods¹, T. Wright¹⁶, and P. Žugec^{17,4}

¹School of Physics and Astronomy, University of Edinburgh, United Kingdom

²Physikalisch-Technische Bundesanstalt (PTB), Bundesallee 100, 38116 Braunschweig, Germany

³CEA Irfu, Université Paris-Saclay, F-91191 Gif-sur-Yvette, France

⁴European Organization for Nuclear Research (CERN), Switzerland

⁵Paul Scherrer Institut (PSI), Villigen, Switzerland

⁶Charles University, Prague, Czech Republic

⁷Universidad de Sevilla, Spain

⁸Goethe University Frankfurt, Germany

⁹Istituto Nazionale di Fisica Nucleare, Sezione di Bologna, Italy

¹⁰Dipartimento di Fisica e Astronomia, Università di Bologna, Italy

¹¹University of Lodz, Poland

¹²Institut de Physique Nucléaire, CNRS-IN2P3, Univ. Paris-Sud, Université Paris-Saclay, F-91406 Orsay Cedex, France

¹³TU Wien, Atominstytut, Stadionallee 2, 1020 Wien, Austria

¹⁴Centro de Investigaciones Energéticas Medioambientales y Tecnológicas (CIEMAT), Spain

¹⁵Istituto Nazionale di Fisica Nucleare, Sezione di Bari, Italy

¹⁶University of Manchester, United Kingdom

¹⁷Department of Physics, Faculty of Science, University of Zagreb, Zagreb, Croatia

¹⁸University of York, United Kingdom

¹⁹University of Santiago de Compostela, Spain

²⁰Universitat Politècnica de Catalunya, Spain

²¹INFN Laboratori Nazionali del Sud, Catania, Italy

²²Dipartimento Interateneo di Fisica, Università degli Studi di Bari, Italy

²³Instituto de Física Corpuscular, CSIC - Universidad de Valencia, Spain

²⁴Instituto Superior Técnico, Lisbon, Portugal

²⁵Horia Hulubei National Institute of Physics and Nuclear Engineering, Romania

²⁶Japan Atomic Energy Agency (JAEA), Tokai-Mura, Japan

²⁷European Commission, Joint Research Centre (JRC), Geel, Belgium

²⁸Karlsruhe Institute of Technology, Campus North, IKP, 76021 Karlsruhe, Germany

²⁹National Technical University of Athens, Greece

³⁰Agenzia nazionale per le nuove tecnologie (ENEA), Italy

³¹INFN Laboratori Nazionali di Legnaro, Italy

³²Consiglio Nazionale delle Ricerche, Bari, Italy

³³Istituto Nazionale di Fisica Nucleare, Sezione di Trieste, Italy

³⁴Department of Physics and Astronomy, University of Catania, Italy

³⁵University of Ioannina, Greece

³⁶University of Vienna, Faculty of Physics, Vienna, Austria

³⁷University of Granada, Spain

³⁸Department of Physics, University of Basel, Switzerland

³⁹Centre for Astrophysics Research, University of Hertfordshire, United Kingdom

⁴⁰Bhabha Atomic Research Centre (BARC), India

⁴¹Australian National University, Canberra, Australia

Abstract. The slow neutron capture process (*s*-process) is responsible for producing about half of the elemental abundances heavier than iron in the universe. Neutron capture cross sections on stable isotopes are a key nuclear physics input for *s*-process studies. The $^{72}\text{Ge}(n, \gamma)$ Maxwellian-Averaged Cross Section (MACS) has an important influence on the production of isotopes between Ge and Zr in the weak *s*-process in massive stars and so far only theoretical estimations are available. An experiment was carried out at the neutron time-of-flight facility n_TOF at CERN to measure the $^{72}\text{Ge}(n, \gamma)$ reaction for the first time at stellar neutron energies. The capture measurement was performed using an enriched $^{72}\text{GeO}_2$ sample at a flight path length of 184 m, which provided high neutron energy resolution. The prompt gamma rays produced after neutron capture were detected with a set of liquid scintillation detectors (C_6D_6). The neutron capture yield is derived from the counting spectra taking into account the neutron flux and the gamma-ray detection efficiency using the Pulse Height Weighting Technique. Over 70 new neutron resonances were identified, providing an improved resolved reaction cross section to calculate experimental MACS values for the first time. The experiment, data analysis and the new MACS results will be presented including their impact on stellar nucleosynthesis, which was investigated using the post-processing nucleosynthesis code *mppnp* for a 25 solar mass model.

1 Introduction

The element production in the universe is a key question and drives the field of nuclear astrophysics since many decades. Neutron capture reactions are the main mechanism for the origin of heavier elements in the universe. Half of the elemental abundances heavier than iron are produced via the slow neutron capture process (*s*-process), which occurs in different burning stages of stars with low neutron densities of 10^7 to 10^{12} cm^{-3} [1, 2]. The resulting neutron capture rates are usually smaller than the beta-decay rates of the unstable reaction products. This forces the reaction path on the nuclear chart along the so-called 'valley of stability'. Therefore, neutron capture cross sections on stable isotopes are a key nuclear physics input for *s*-process studies. More precisely, Maxwellian-averaged cross sections (MACS) are used, as the neutron capture cross section is averaged over the stellar neutron velocity distribution of a certain stellar temperature kT , where the reaction takes place.

Elements between mass number 60 and 90 are mainly produced by an *s*-process component which occurs in massive stars during He core burning (0.3 GK) and during C-shell burning (1 GK). Neutron exposures are too low to establish a reaction flow equilibrium [2]. Therefore, the neutron capture cross sections directly influence the abundances and are important to be measured precisely. Unfortunately, some intermediate mass nuclei like ^{72}Ge , still rely on theoretical cross sections based on scarce nuclear data, if one studies the database of KADoNiS-v0.3 [3]. Furthermore, the recommended theoretical MACS value for $^{72}\text{Ge}(n, \gamma)$ between 59 mb [4] and 73 mb [3] can have realistic uncertainties of up to 25%, taking the wide spread of predictions into account. This proceeding reports on the $^{72}\text{Ge}(n, \gamma)$ measurement performed at n_TOF. Lastly, there are more capture cross section results on other stable germanium isotopes from n_TOF recently [5–7].

*e-mail: mirco.dietz@ptb.de

2 Experiment

The experiment was performed at the neutron time-of-flight facility n_TOF at CERN. At n_TOF, highly energetic protons (20 GeV/c) from the CERN Proton Synchrotron (PS), 10^{12} particles in a bunch, impinge on the 1.3 tonne lead target and spallation reactions occur. The surrounding water layers of few cm cool the target and act as a moderator for the high energy neutrons. This results in a wide neutron energy spectrum over up to 12 orders of magnitude from several GeV down to 25 meV. The measurement in the Experimental ARa 1 (EAR-1) with a flight path of 183.96(4) m exploited the excellent neutron energy resolution [8].

The detector setup consisted of four liquid C_6D_6 scintillators (1 liter deuterated benzene each), optimized with Carbon fibre housing for low neutron sensitivity. The detectors were installed 7.7 cm upstream the sample under backwards angle of 125° to register the prompt γ -rays from the capture reaction. The capture sample with a diameter of 2 cm and a mass of 2.68 g was made from 96.59% enriched $^{72}\text{GeO}_2$ powder. Additional samples like Au and metallic natural germanium were used for comparison purposes and an empty sample for background estimation.

The neutron flux was measured extensively in a dedicated campaign during commissioning runs using different detectors system exploiting neutron standard cross sections on ^6Li and ^{235}U . More details on the neutron flux monitoring can be found in Ref. [9].

3 Data Analysis

At n_TOF, we study time and amplitude correlated signals of capture events to determine neutron energy dependent capture cross sections. Initial steps like stability checks, time-of-flight to neutron energy conversion (E_n) or the energy calibration of the C_6D_6 amplitude signals are de-

scribed in details in [10]. The capture yield Y was calculated via

$$Y(E_n) = f_N(E_n) \frac{C_w(E_n) - B_w(E_n)}{\Phi_n(E_n)}, \quad (1)$$

with weighted capture counting spectra (C_w), its background correction (B_w) and the neutron flux ($\Phi_n(E_n)$). The factor f_N reflects a normalization procedure with a thin gold sample exploiting the saturated resonance method [11] for the 4.9 eV resonance in $^{197}\text{Au}(n, \gamma)$. The efficiency of the detector setup is taken into account by the Pulse Height Weighting Technique [12], which includes detailed Geant4 simulations and certain assumptions on the detection technique chosen. A detailed description, the weighting factors and further small correction factors are given in [10].

4 Results

In total, 93 resonances from $^{72}\text{Ge}(n, \gamma)$ were identified and resolved in the neutron energy region up to 43 keV with 77 new resonances, which were not known in any database before. In general, capture data are not sensitive to individual decay widths such as the gamma width Γ_γ or the neutron width Γ_n , but to the kernel of a resonance $K = g \frac{\Gamma_\gamma \Gamma_n}{\Gamma_\gamma + \Gamma_n}$ with the spin factor g . The kernel data up to 43 keV, derived from the capture yield with R-Matrix code SAMMY, was presented in [13] and the data is available on EXFOR [14]. Moreover, an averaged cross section between 43 keV and 300 keV was provided in EXFOR as well.

Here, we provide the neutron capture cross section on ^{72}Ge from 30 eV to 330 keV in Figure 1, which summarises our findings in the resolved and unresolved energy region. Furthermore, Figure 1 shows a comparison with data from ENDF/B-VIII.0 evaluation [15] and clearly states the improved range of resolved resonances from 12 keV up to 43 keV with the our data.

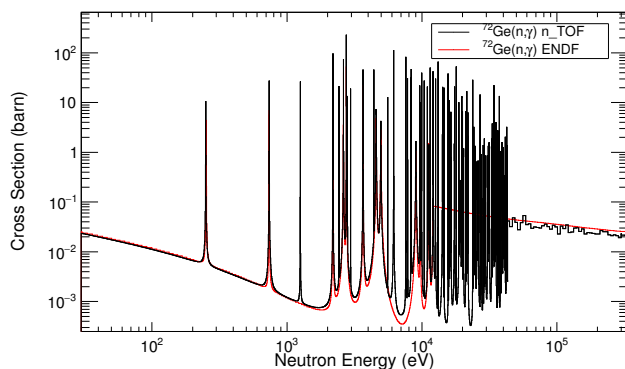


Figure 1. $^{72}\text{Ge}(n, \gamma)$ cross section results are shown in comparison with the evaluation of ENDF/B-VIII.0 [15]. Numerous new resonance data in the keV region extends the resolved resonance data from 12 keV in ENDF to 43 keV.

The Maxwellian-averaged cross sections of $^{72}\text{Ge}(n, \gamma)$ between 5 keV and 100 keV were derived via

$$\text{MACS} = \frac{2}{\sqrt{\pi}} \frac{1}{(kT)^2} \int_0^\infty \sigma(E_n) \cdot E_n \cdot \exp\left(-\frac{E_n}{kT}\right) dE_n \quad (2)$$

from the new capture cross section and scaled ENDF cross section above 300 keV, which only has minor contribution for $kT \geq 50$ keV. The MACS results are shown in Figure 2 in comparison to values of KADoNiS-v0.3 [3]. The same energy dependence of the MACS is observed, but the n_TOF results are between 17% and 24% lower database values. Moreover, the new results exhibit only relative uncertainties between 3.2% and 7.1%, which marks a significant improvements to the 'theoretical' evaluation before. An detailed budget of the different sources of statistical and systematic uncertainties is described in [10]. Finally, the result at $kT = 30$ keV with 57.4 ± 3.0 mb has a total uncertainty under 5%, which is the general target for input data on stellar models.

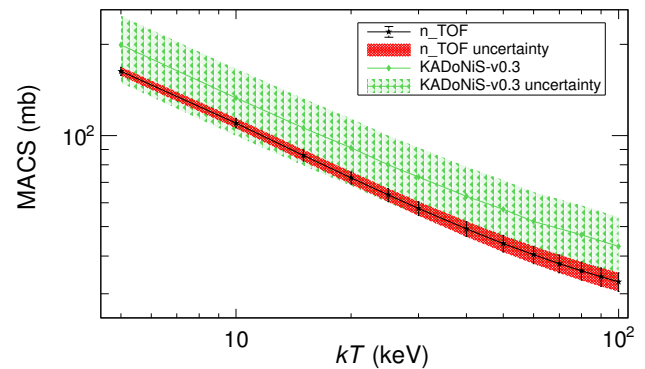


Figure 2. MACS values for kT from 5 keV to 100 keV are shown in comparison with the KADoNiS database [3] and a difference of about 20% is observed on average. Uncertainties are displayed in shaded area with 25% assumed for the KADoNiS values. Clearly, the n_TOF result brings a significant improvement with uncertainties below 5% for $kT \leq 30$ keV.

5 Astrophysical Implication

The implication of the new cross section result was investigated using a 25 solar mass star with 2% metallicity, modelled with the code MESA [16]. The post-processing code mppnp [17] replicated the s -process nucleosynthesis. Abundances were calculated with different cross section inputs for $^{72}\text{Ge}(n, \gamma)$, comparing n_TOF and KADoNiS-v0.3 values. The resulting ratios for the two main stellar regions are shown in Figure 3 and more details on the stellar conditions can be found in [10]. The abundance ratio changes up to 20% or 25%, which is similar in He core ($kT = 26$ keV) and C shell ($kT = 90$ keV), as there is a consistent difference of about 20% between the MACS from KADoNiS-v0.3 and n_TOF for all stellar temperatures.

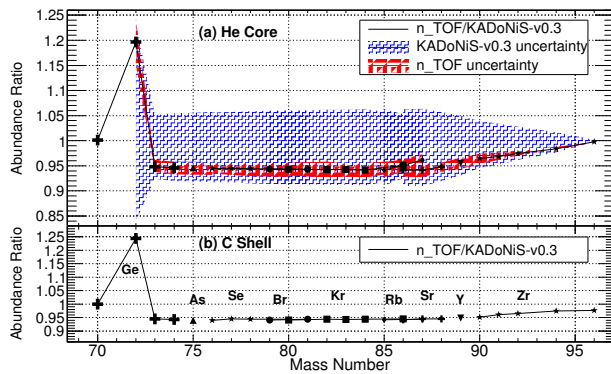


Figure 3. *s*-process abundances from the 25 solar mass star model ($Z=0.02$) using the new cross section results from n_TOF , are normalised to results using the $^{72}\text{Ge}(n, \gamma)$ MACSs from the recommendation of KADoNiS-v0.3 [3]. Isotopes of the same elements (labelled by symbol) are connected by thin solid lines. Panel (a) displays the ratio of abundances after He-core burning. The shaded areas estimate abundance variations when taking into account uncertainties of KADoNiS (blue) or n_TOF (red) cross sections. The abundance uncertainties are significantly reduced by the improved cross section results. Panel (b) shows abundances of the later C-shell burning phase.

In conclusion, we have measured the $^{72}\text{Ge}(n, \gamma)$ cross section with high precision at the CERN n_TOF facility for the first time, and covered a wide neutron energy range relevant for *s*-process nucleosynthesis. The results drastically reduce uncertainties in the calculation of abundances produced via the *s*-process in He-core and C-shell burning phases in massive stars.

In line with the principles that apply to scientific publishing and the CERN policy in matters of scientific publications, the n_TOF Collaboration recognises the work of V. Furman and P. Sedyshev (JINR, Russia), who have contributed to the experiment used to obtain the results described in this paper. This work was supported by the European Research Council ERC-2015-STG Nr. 677497, the Austrian Science Fund FWF (J 3503), the Science and Technology Facilities Council UK (ST/M006085/1), the Adolf Messer Foundation, the Croatian Science Foundation under the project 8570, the MSMT of the Czech Re-

public, the Charles University UNCE/SCI/013 project and by the funding agencies of the participating institutes.

References

- [1] R. Reifarth, C. Lederer, and F. Käppeler, *J. Phys. G* **41**, 053101 (2014)
- [2] M. Pignatari *et al.*, *The Astroph. J.* **33**, 1557-1577 (2010)
- [3] I. Dillmann *et al.*, *AIP Conf. Proc.*, **819(1)**, 123-127 (2006)
- [4] I. Dillmann *et al.*, *Nucl. Data Sheets* **120**, 171-174 (2014), <http://www.kadonis.org>
- [5] C. Lederer-Woods *et al.* (n_TOF Collaboration), *Phys. Lett. B* **790**, 458 (2019)
- [6] A. Gawlik *et al.* (n_TOF Collaboration), *Phys. Rev. C* **100**, 045804 (2019)
- [7] A. Gawlik-Ramięga *et al.* (n_TOF Collaboration), *Phys. Rev. C* **104**, 044610 (2021)
- [8] C. Guerrero *et al.* (n_TOF Collaboration), *Eur. Phys. J. A* **49**, 27 (2013)
- [9] M. Barbagallo *et al.* (n_TOF Collaboration), *Eur. Phys. J. A* **49**, 156 (2013)
- [10] M. Dietz, *Measurement of the $^{72}\text{Ge}(n, \gamma)$ cross section at n_TOF CERN over a wide energy range and Implications for stellar Nucleosynthesis* (PhD Thesis, Edinburgh, 2021)
- [11] R. L. Macklin *et al.*, *Nucl. Instrum. Methods A* **164**, 213 (1979)
- [12] U. Abbondanno *et al.* (n_TOF Collaboration), *Nucl. Instr. Meth. Phys. Res. A* **521**, 454-467 (2004)
- [13] M. Dietz *et al.* (n_TOF Collaboration), *Phys. Rev. C* **103**, 045809 (2021)
- [14] M. Dietz *et al.*, EXFOR Entry 23757004 (2021)
- [15] D. A. Brown *et al.*, *Nucl. Data Sheets* **148**, 1-142 (2018)
- [16] C. Ritter *et al.*, *Mon. Not. R. Astron. Soc.* **480**, 538 (2018)
- [17] M. Pignatari *et al.*, *The Astroph. J., Suppl. Ser.* **225**, 24 (2016)